Distributed Control, Load Sharing, and Dispatch in DC Microgrids

Jinxin Zhao and Florian Dörfler

Abstract— **Due to their compatibility with distributed generation microgrids are a promising operational architecture for future power systems. Here we consider the operation of DC microgrids that arise in many applications. We adopt a linear circuit model and propose a novel decentralized voltage droop control strategy inspired by frequency droop in AC networks. In comparison to conventional DC voltage droop strategies, our novel droop controller is able to achieve load sharing (even in presence of actuation constraints) or an optimal economic generation dispatch. Similar to AC frequency droop control, our voltage droop control induces a steady-state voltage drift as global signal depending on load/generation imbalance. Thus, we augment the primary droop controller with additional secondary regulation and investigate two strategies: a fully decentralized secondary integral control strategy successfully compensates for the steady-state voltage drifts yet it fails to achieve the desired optimal steady-state injections. Next, we propose a consensus filter that requires communication among the controllers, that regulates the voltage drift, and that recovers the optimal injections. The performance and robustness of our controllers are illustrated through simulations.**

I. Introduction

Driven by environmental concerns, renewable energy sources are rapidly deployed, such as photovoltaic and wind generation. These sources will, for the most part, be deployed as small-scale sources in low-voltage distribution networks. As a consequence, the conventional centralized operation of power grids is advancing towards a distributed architecture.

Microgrids are low-voltage electrical networks that have been proposed as a conceptual architecture to operate distributed generations, storages and loads. The advantages of microgrids are as follows: First, they are capable of connecting to the larger utility grid but also able to island themselves and operate independently, e.g., in case of an outage. Second, microgrids can be deployed as stand-alone small-footprint systems (possibly in remote locations) while providing high quality power supply, e.g., in third-world villages but also in hospitals, military bases, or universities. Third and finally, microgrids are naturally designed to integrate small-scale distributed generation, that is, power is generated where it is needed without transmission and distribution losses.

Microgrids have been proposed based on either alternative current (AC) or direct current (DC). AC power grids have been in service for many decades, and their components and operation are well understood. The operational paradigms from conventional AC power transmission networks have been inherited in AC microgrids [1]. However, using DC microgrids has the following advantages: There is an increasing number of DC sources and storages (e.g., solar cells and Li-ion batteries), end-user equipment (e.g., electric vehicles), and most of the contemporary electronic appliances. In [2] it is demonstrated that most of the loads supplied by AC nowadays can operate well with a DC supply. Moreover, the efficiency is raised, because of the reduction of conversion losses of inverters between AC and DC. Finally, DC microgrids are widely deployed in aircrafts and spacecrafts [3]. In summary, DC microgrids are a promising technology that has already attracted much research attention.

Jinxin Zhao is with the Department of Mechanical and Aerospace Engineering, University of California, Los Angeles, California, 90024. Email: jinxinzh@ucla.edu. Florian Dörfler is with the Automatic Control Laboratory, Swiss Federal Institute of Technology (ETH) Zürich, Switzerland, 8044. Email: dorfler@ethz.ch.

Literature review: In [4], a modeling method of a single DC microgrid cluster is described. A hierarchical control layout for DC microgrids is proposed in [1]: a primary controller rapidly stabilizes the grid, and a secondary controller (on a slower time scale) corrects for the steady-state error induced by primary control. An experimental system involving solar-cell, wind turbine and power storage is designed and constructed in [5]. A low-voltage DC distribution system for sensitive loads is described in [6]. These works focus on the hardware implementation of DC microgrids. A scenario-based operation strategy for a DC microgrid is developed in [7] based on detailed wind turbine and battery models. A cooperative control paradigm is proposed in [8] to establish a distributed secondary/primary control framework for DC microgrid requiring communication capabilties. Distributed controllers have been studied to regulate multi-terminal DC transmission systems which share similar problem aspects with DC microgrids. The controller proposed in [9] achieves fair power sharing and asymptotically minimizes the cost of the power injections. In [10] a unified port-Hamitonian system model is proposed, and the performance of decentralized PI control is discussed for a multi-terminal DC transmission system. For AC microgrids a flat and distributed operation architecture has been proposed in [11], [12], consisting simultaneous (without time-scale separation) primary, secondary, and tertiary control. Inspired by these AC operation strategies we seek similar solutions for DC microgrids.

Contribution and contents: In this article, we propose a comprehensive operational control strategy for DC microgrids in order to achieve multiple objectives. Aside from the importance of DC microgrids in their own right, we believe that our article also serves as valuable tutorial that illustrates many power system operational paradigms in a linear setting that have nonlinear parallels in AC networks.

In Section III, we introduce the considered DC microgrid model. Here we consider a purely resistive network with constant current loads, and we refer to [13] for more detailed network and load models. Inspired by the shortcomings of conventional DC droop control and the merits of frequency droop control in AC systems, we propose a novel primary voltage droop control strategy in Section IV. Our controller is fully decentralized and capable of stabilizing the grid while achieving load sharing and avoiding actuator saturation.

In Section V, we consider the optimal economic dispatch of multiple generating units. We demonstrate that the optimal injections (according to the economic dispatch) are in one-to-one correspondence with the steady state injections achieved by our primary voltage droop control with appropriately chosen control gains. As a result, we propose a selection of control gains to achieve economic optimality in a fully decentralized way and without a model of the microgrid.

In Section VI, we discuss the limitations of droop control causing steady-state voltage drifts and study secondary control strategies to compensate for it. First, we consider a fully decentralized integral control strategy and illustrate its limitations. Next, we propose a distributed consensus filter that relies on communication between local controllers. We show that this distributed control strategy is capable of regulating the voltage drifts while simultaneously achieving tertiary-level objectives such as load sharing or economic dispatch.

In Section VII, we present simulation results to illustrate the performance and robustness of our controllers.

Finally Section VIII concludes the paper. Due to space limitations, we omit most proofs and refer to [13] for details.

II. Preliminaries and Notation

Vectors and matrices: Let $\mathbf{1_n}$ and $\mathbf{0_n}$ be the n-dimensional vectors of unit and zero entries, respectively. Let $\mathbf{I_n} \in \mathbb{R}^{n\times n}$ be the n-dimensional identity. Let $\mathbf{diag}(v)$ represent a diagonal matrix with the elements of v on the diagonal. For a symmetric matrix $A = A^T$, the notation $A > 0$, $A \geq 0$, $A < 0$, and $A \leq 0$ means that A is positive definite, positive semidefinite, and negative definite and negative semidefinite, respectively.

Algebraic graph theory: Consider a connected, undirected, and weighted graph $G = (\mathcal{V}, \mathcal{E}, W)$, where $\mathcal{V} = \{1, ...n\}$ is the set of nodes, $\mathcal{E} \subset \mathcal{V}\times\mathcal{V}$ is the set of undirected edges, and $W = W^T \in \mathbb{R}^{n\times n}$ is the adjacency matrix with entries $w_{ij} > 0$ for $(i, j) \in \mathcal{E}$ and $w_{ij} = 0$ otherwise. The degree matrix $D \in \mathbb{R}^{n\times n}$ is a diagonal matrix with elements $d_{ii} = \sum_{j=1,j\neq i}^{n} w_{ij}$. The Laplacian matrix $L = L^T = D - W \in \mathbb{R}^{n\times n}$ satisfies $L \geq 0$ and $L\mathbf{1_n} = \mathbf{0_n}$. For a connected graph the null space of L is spanned by $\mathbf{1_n}$ and all other $n - 1$ eigenvalues of L are strictly positive.

III. DC Microgrid Model

For our purposes a microgrid is a linear connected circuit with associated undirected graph $G(\mathcal{V}, \mathcal{E}, W)$, nodes $\mathcal{V} = \{1, ..., n\}$, and edges $\mathcal{E} \subset \mathcal{V} \times \mathcal{V}$. We assume that all lines in the DC microgrid are purely resistive, and refer to [13] for an extension of our results towards more general line models. The nonzero entries of the adjacency matrix W are $w_{ij} = w_{ji} = 1/R_{ij}$, where R_{ij} is the resistance of the line connecting nodes $i, j \in \mathcal{V}$. The diagonal degree matrix $D \in \mathbb{R}^{n\times n}$ has elements $d_{ii} = \sum_{j=1,j\neq i}^{n} w_{ij}$. The admittance matrix Y is defined as $Y = D-W$. Thus, $Y = Y^T \in \mathbb{R}^{n\times n}$ is a real-valued Laplacian matrix satisfying $\mathbf{1}_n^T Y = \mathbf{0}_n^T$.

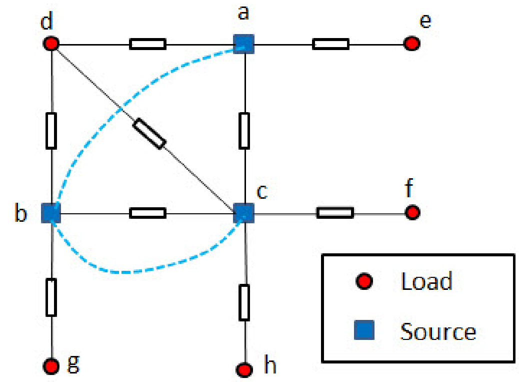

Fig. 1. A DC Microgrid with three sources and five loads. The blue dashed lines indicate the communication among the controllers (18) in Section VI.

We partition the set of nodes into m sources and $n - m$ loads: $\mathcal{V} = \mathcal{V}_S \cup \mathcal{V}_L$. Throughout this paper we denote sources and loads by the subscripts S and L, respectively. The sources are assumed to be controllable current sources with positive current injections $I_i^S \geq 0$ and are assembled in the vector I^S. Each source is constrained by its output current capacity $\bar{I}_i$, i.e., $I_i^S \in [0, \bar{I}_i]$. The loads are assumed to be constant-current loads with negative current injections $I_i^L \leq 0$ and are assembled in the vector I^L.[1] Following Kirchhoff's and Ohm's laws, the network model is built as

$$\begin{bmatrix} I^S \\ I^L \end{bmatrix} = \begin{bmatrix} Y_{SS} & Y_{SL} \\ Y_{SL}^T & Y_{LL} \end{bmatrix} \begin{bmatrix} V^S \\ V^L \end{bmatrix} \tag{1}$$

where the admittance matrix Y is partitioned accordingly, and V^S and V^L represent the nodal voltages (potentials) of sources and loads, respectively. Figure 1 shows an example network of a DC microgrid. Since Y is a Laplacian matrix, a necessary feasibility condition for equation (1) is

$$\mathbf{1}_m^T I^S + \mathbf{1}_{n-m}^T I^L = 0, \tag{2}$$

that is, load and generation need to be balanced. Observe that this constraint cannot be satisfied since the generation needs to be scheduled to meet the generally unknown load. This observation motivates primary control actions akin to AC systems that instantaneously balance generation and load.

IV. Primary Droop Control & Load Sharing

We briefly review *frequency droop control* in AC microgrids [1] to motivate our proposed control strategy for DC microgrids. In AC microgrids the active power injection P_i at source i is controlled to be proportional to its frequency deviation $\dot{\theta}_i$ (from a nominal frequency) as

$$P_i = P_i^* - C_i\dot{\theta}_i, \tag{3}$$

[1]Loads in DC systems are conventionally modeled as constant current/impedance/voltage/power loads [2] and often display a combination of the above properties. Here we focus on constant-current loads which arise primarily in electronic loads and also in LED lighting. We find that these loads are the mathematically most challenging linear load models. In [13] we extend our results to constant-impedance loads and constant-voltage buses.

where the control gain $C_i > 0$ is referred to as the droop coefficient, $P_i^* \in [0,\ \bar{P}_i]$ is a nominal injection setpoint, and $\bar{P}_i$ is the capacity of source i. For a particular selection of droop coefficients, it can be shown that frequency droop control stabilizes the AC microgrid to a synchronous solution and achieves proportional load sharing at steady state [12], that is, every source i injects active power P_i according its capacity $\bar{P}_i$: $P_i/\bar{P}_i = P_j/\bar{P}_j$ for all sources $i, j \in \mathcal{V}_S$. A key feature of AC frequency droop control is that it synthesizes the synchronous frequency as a global signal indicating the load/generation imbalance in the microgrid [11], [12].

As for AC systems, a primary control objective in DC microgrids is to design local decentralized droop controllers that achieve *proportional load sharing* in the sense that

$$I_i^S/\bar{I}_i = I_j^S/\bar{I}_j \quad \text{for all } i, j \in \mathcal{V}_S\,, \tag{4}$$

where $I_i^S \in [0, \bar{I}_i]$ is the current injection of source $i \in \mathcal{V}_S$ and $\bar{I}_i > 0$ is its capacity. The conventional *DC voltage-vs-current droop controller* is given by (see, e.g., [10], [8], [4])

$$I_i^S = I_i^* - C_i V_i^S, \tag{5}$$

where $I_i^* \in [0, \bar{I}_i]$ is an injection setpoint and the gain $C_i > 0$ is referred to as *droop coefficient*. Unless non-local (distributed or centralized) secondary controllers or carefully tuned virtual impedance controllers are added, the controller (5) does generally not achieve load sharing (especially for non-negligible line impedances); see [8] for a review. From a mathematical perspective this shortcoming is essentially due to the absence of a global variable such as the AC frequency.

Here we start from the observation that the conventional controller (5) can be interpreted as the steady-state of the following proportional-integral droop controller:

$$I_i^S = I_i^* - C_i \dot{V}_i^S - p_i\,, \tag{6a}$$

$$D_i \dot{p}_i = \dot{V}_i^S\,. \tag{6b}$$

Observe that (6a) mimics the AC frequency droop (3) and (6b) is an integral controller compensating for steady-state drifts similar to a decentralized secondary frequency integral controller often added to droop in AC systems. Inspired by this observation, the success of frequency droop control (3) in AC systems, and the limitation of conventional DC droop control (5), we propose the *primary voltage droop controller*

$$\boxed{I_i^S = I_i^* - C_i \dot{V}_i^S}\,. \tag{7}$$

Fig. 2 shows a circuit realization of our droop controller (7) via a constant current source I_i^* and a shunt capacitance C_i reminiscent of standard shunt compensation in DC power systems [14]. The proposed primary droop control (7) is a fully decentralized and proportional control strategy.

Similar to AC droop control (3), our controller (7) induces a global variable, namely a constant voltage drift, that depends on the total imbalance in load/generation current injections: $\sum_{j\in\mathcal{V}_S} I_j^* + \sum_{j\in\mathcal{V}_L} I_j^L$. Of course, this drift has to be compensated by a secondary controller, which will be done in Section VI. Before that we will analyze the primary droop control loop (1) and (7) by itself and show, among others, that it achieves stable proportional load sharing:

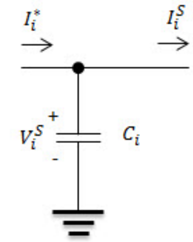

Fig. 2. Realization of droop control (7) as analog circuit

Theorem 4.1: (Primary control & load sharing) *Consider the closed-loop droop-controlled microgrid* (1) *and* (7). *Then the following statements hold:*

(1) Voltage drifts: *all voltages V_i^S, $i \in \mathcal{V}_S$ converge exponentially to $V(t) = V^* + \dot{v}_{\text{drift}} t \cdot \mathbf{1}_m$, where $V^* \in \mathbb{R}^m$ is a constant vector and the common voltage drift is*

$$\dot{v}_{\text{drift}} = \frac{\sum_{j\in\mathcal{V}_S} I_j^* + \sum_{j\in\mathcal{V}_L} I_j^L}{\sum_{j\in\mathcal{V}_S} C_j}\,. \tag{8}$$

(2) Proportional load sharing: *if the droop coefficients and nominal injection setpoints are selected proportionally, that is, for all $i, j \in \mathcal{V}_S$*

$$C_i/\bar{I}_i = C_j/\bar{I}_j \quad \textit{and} \quad I_i^*/\bar{I}_i = I_j^*/\bar{I}_j, \tag{9}$$

then at steady state the load is shared proportionally.

Proof: The closed-loop state space model (1), (7) is

$$\begin{bmatrix} C\dot{V}^S \\ 0 \end{bmatrix} = \begin{bmatrix} I_S^* \\ I^L \end{bmatrix} - \begin{bmatrix} Y_{SS} & Y_{SL} \\ Y_{SL}^T & Y_{LL} \end{bmatrix} \begin{bmatrix} V^S \\ V^L \end{bmatrix}, \tag{10}$$

where $C = \mathbf{diag}(C_1, ..., C_m)$. Since Y_{LL} is invertible [15, Lemma II.1], we eliminate the variable $V^L = Y_{LL}^{-1}(I^L - Y_{SL}^T V^S)$. from the second block of (algebraic) equations in (10). This elimination process, termed Kron-reduction in circuit theory [15], gives the Kron-reduced system

$$\dot{V}^S = -C^{-1}\tilde{L}V^S + C^{-1}\tilde{I} \tag{11}$$

where $\tilde{I} = I_S^* - Y_{SL}Y_{LL}^{-1}I^L$ and $\tilde{L} = Y_{SS} - Y_{SL}Y_{LL}^{-1}Y_{SL}^T$ is again a positive semidefinite Laplacian [15, Lemma II.1]. By Sylvester's Law of Inertia [16, Corollary 3], because $C^{-1} > 0$ and $\tilde{L}$ is symmetric, $C^{-1}\tilde{L}$ has the same number of negative, zero and positive eigenvalues as $\tilde{L}$. Thus, $C^{-1}\tilde{L}$ has one zero-eigenvalue and all other eigenvalues are positive. The right eigenvector associated to the zero eigenvalue is $\mathbf{1}_m$.

It follows that all modes in the Kron-reduced system (11) exponentially decay to zero with exception of the zero mode with right eigenvector $\mathbf{1}_m$ and left eigenvector $C\mathbf{1}_m$. Hence, this zero mode is simply integrated and all components of the vector $\dot{V}_S$ will asymptotically have the same value $\dot{v}_{\text{drift}}$. We project the differential-algebraic equations (10) onto the zero mode by summing all equations (10) as $\mathbf{1}_m^T C\dot{V}_S = \mathbf{1}_m^T I^S + \mathbf{1}_{n-m}^T I^L$. In steady state for $\dot{V}_S = \dot{v}_{\text{drift}}\mathbf{1}_m$, we recover the voltage drift (8). This proves statement (1).

At steady state, the closed-loop injections are

$$I_i^S = -C_i\dot{v}_{\text{drift}} + I_i^*. \tag{12}$$

Thus, $I_i^S/\bar{I}_i = (-C_i\dot{v}_{\text{drift}} + I_i^*)/\bar{I}_i$. The proportional load sharing objective $I_i^S/\bar{I}_i = I_j^S/\bar{I}_j$ (for all $i, j \in \mathcal{V}_S$) can be achieved by choosing I_i^* and C_i proportionally as in (9). This proves statement (2) of Theorem 4.1. ■

Theorem 4.1 gives a criterion for stable load sharing of the closed-loop system (1), (7), namely the droop coefficients need to be picked proportional to capacity $C_i = \gamma \bar{I}_i$, where $\gamma > 0$ is constant. However, Theorem 4.1 does not guarantee that the injections satisfy the actuation constraint $I_i \in [0, \bar{I}_i]$. If the control gains are chosen as in (9), then the actuation constraint is met if and only if the total load $\sum_{j\in\mathcal{V}_L} I_j^L$ can be satisfied by the maximal injections (at capacity) $\sum_{i\in\mathcal{V}_S} \bar{I}_i$.

Theorem 4.2 (Actuation constraints): *Consider a stationary solution of the closed-loop system* (1) *and* (7) *with droop coefficients and setpoints chosen proportionally as in* (9). *The following statements are equivalent:*

(1) Injection constraints: $0 \leq I_i^S \leq \bar{I}_i$ *for all* $i \in \mathcal{V}_S$*;*

(2) Load satisfiability: $\sum_{i\in\mathcal{V}_S} \bar{I}_i \geq -\sum_{j\in\mathcal{V}_L} I_j^L \geq 0$.

Proof: The steady-state injection is given by (8) and (12). The condition $I_i^S \geq 0$ for each $i \in \mathcal{V}_S$ translates to

$$I_i^S = I_i^* - C_i \frac{\sum_{j\in\mathcal{V}_S} I_j^* + \sum_{k\in\mathcal{V}_L} I_k^L}{\sum_{j\in\mathcal{V}_S} C_j} \geq 0.$$

For proportional coefficients (9), we have $C_i/I_i^* = C_j/I_j^*$ and the previous inequality equivalently reads as

$$\sum\nolimits_{k\in\mathcal{V}_L} I_k^L \leq -\sum\nolimits_{j\in\mathcal{V}_S} \left(I_j^* - C_j \frac{I_i^*}{C_i} \right) = 0.$$

A similar calculation, for $I_i^S \leq \bar{I}_i$, for $i \in \mathcal{V}_S$, yields

$$I_i^S = I_i^* - C_i \frac{\sum_{j\in\mathcal{V}_S} I_j^* + \sum_{k\in\mathcal{V}_L} I_k^L}{\sum_{j\in\mathcal{V}_S} C_j} \leq \bar{I}_i.$$

The coefficients satisfy $C_i/(\sum_{j\in\mathcal{V}_j} C_j) = \bar{I}_i/(\sum_{j\in\mathcal{V}_j} \bar{I}_j) = I_i^*/(\sum_{j\in\mathcal{V}_j} I_j^*)$, thus the previous inequality also reads as

$$\sum_{k\in\mathcal{V}_L} I_k^L \geq (I_i^* - \bar{I}_i) \frac{\sum_{j\in\mathcal{V}_j} C_j}{C_i} - \sum_{j\in\mathcal{V}_j} I_j^* = -\sum_{j\in\mathcal{V}_S} \bar{I}_j.$$

These inequalities complete the proof of Theorem 4.2. ■

We conclude that our primary droop controller (7) achieves stable proportional load sharing in a fully decentralized way and while respecting actuation constraints. However, as in AC systems, the droop controller (7) induces a steady-state voltage drift (8) which is proportional to the total injection imbalance $\sum_{j\in\mathcal{V}_S} I_j^* + \sum_{j\in\mathcal{V}_L} I_j^L$. This imbalance is zero only if a precise forecast of the total load $\sum_{j\in\mathcal{V}_L} I_j^L$ is known and the nominal injections I_i^* can be scheduled accordingly. Such a precise forecast is generally not available, the nominal injections are fixed (typically to 0 or $\bar{I}_i$), and the loads are changing with time. Another way to reduce the voltage drift $\dot{v}_{\text{drift}}$ in (8) is to choose large droop coefficients $C_i \gg 1$. The latter choice is not viable since it results in a slow *sluggish* control response. We will address the issue of regulating the voltage drift in Section VI. Before that we will address the *tertiary control* (or energy management) problem.

V. Optimal Economic Dispatch & Droop Control

The proportional droop coefficients (9) lead to fair load sharing (4) among the sources proportional to their capacity. However, this objective may not be desirable when sources rely on different energy generation and conversion mechanisms, e.g., solar cells have lower capacities compared with diesel generators, but they may be preferred for economic and environmental reasons. In the following, we consider an alternative generation dispatch criterion, namely the *economic dispatch* formalized as an optimization problem:

$$\underset{\{u,\ V^S,\ V^L\}}{\text{minimize}} \; f(u) = \sum\nolimits_{i=1}^{m} \frac{1}{2}\alpha_i u_i^2 \tag{13a}$$

$$\text{subject to } \begin{bmatrix} I_S^* + u \\ I^L \end{bmatrix} = Y \begin{bmatrix} V^S \\ V^L \end{bmatrix} \tag{13b}$$

The optimization problem (13) is convex with quadratic objective and linear constraints. The coefficients $\alpha_i > 0$ are reflecting the fuel and operation costs of of power source i , its capacity, or other preferences. In case that the nominal injection setpoints I_i^* are zero, the decision variable u_i equals the total generation of source i. For nonzero setpoints $I_i^* > 0$, u_i is the reserve generation to meet the real-time demand.

Theorem 5.1 (Economic dispatch): *Consider the optimization problem* (13). *The optimal injections are*

$$u_i^* = -c/\alpha_i, \quad i \in \mathcal{V}_s\,, \tag{14}$$

where $c = \frac{\mathbf{1}_m^T I_S^* + \mathbf{1}_{n-m}^T I^L}{\sum_i 1/\alpha_i}$ *is a constant.*

Proof: The Lagrangian associated to (13) is

$$\mathcal{L}(u, V, \lambda) = \sum\nolimits_{i=1}^{m} \frac{1}{2}\alpha_i u_i^2 + \lambda^T \left(\begin{bmatrix} I_S^* + u \\ I^L \end{bmatrix} - YV \right)$$

where $V = \begin{bmatrix} V^S & V^L \end{bmatrix}^T$ and $\lambda = \begin{bmatrix} \lambda^S & \lambda^L \end{bmatrix}^T \in \mathbb{R}^n$.

The KKT conditions $\partial\mathcal{L}/\partial V = 0$, $\partial\mathcal{L}/\partial\lambda = 0$ and $\frac{\partial\mathcal{L}}{\partial u} = 0$ are necessary and sufficient for optimality due to the convexity of (13) [17] . The first condition is $\partial\mathcal{L}/\partial V = -\lambda^T Y = 0$. Since Y is a Laplacian matrix, $\text{null}(Y) = \text{span}(\mathbf{1}_n)$. Thus, we have that $\lambda = c\mathbf{1}_n$, where $c \in \mathbb{R}$ is a constant. The second condition is $\frac{\partial\mathcal{L}}{\partial u} = u^T \mathbf{diag}(\alpha_i) + \lambda_S^T = 0$. It follows that $u_i^* = -c/\alpha_i$. The constraint (13b) implies

$$\mathbf{1}_n^T \begin{bmatrix} I_S^* + u \\ I^L \end{bmatrix} = \mathbf{1}_m^T I_S^* + \mathbf{1}_{n-m}^T I^L + \mathbf{1}_m^T u = \mathbf{1}_n^T YV = 0.$$

Since $u_i^* = -c/\alpha_i$, then $c \sum 1/\alpha_i = (\mathbf{1}_m^T I_S^* + \mathbf{1}_m^T I^L)$. ■

Theorem 5.1 gives the optimal economic dispatch u_i as a function of the nominal injections I_S^*, the (possibly unknown) loads I^L, and the cost coefficients α_i. Observe from (14) that at optimality all marginal costs are identical:

$$\alpha_i u_i^* = \alpha_j u_j^* \quad i \in \mathcal{V}_s\,. \tag{15}$$

Note the similarity between the optimal injections (14) and the steady-state injections of droop-controlled microgrid (8) and (12). Based on this observation, we present the following result: the optimal solution of the economic dispatch (14) can be achieved by an appropriately designed droop control (7). Conversely, any steady state of the droop-controlled microgrid (1) and (7) is the optimal solution of the economic dispatch (14) with appropriately chosen parameters.

Corollary 5.1: (Droop control & economic dispatch) *Consider the following two injections:*
(**1**) *The optimal injection* $I_i^* + u_i^*$ *of the economic dispatch problem* (13) *with cost coefficients* α_i*; and*
(**2**) *The steady-state injections* $I_i^* - C_i \dot{v}_{\text{drift}}$ *of the droop-controlled microgrid* (1) *and* (7) *with droop coefficients* C_i*.*
These two injections are identical if and only if

$$\alpha_i C_i = \alpha_j C_j \quad \text{for all } i, j \in \mathcal{V}_S. \tag{16}$$

Notice that the optimal injection (in the sense of the economic dispatch (13)) can be achieved in a fully decentralized manner, without any communication or a knowledge of the microgrid and the loads when the droop gains are chosen as $C_i = \beta/\alpha_i$ for some constant $\beta > 0$. In general, the optimal droop gain $D_i = \beta/\alpha_i$ and the droop gain $D_i = \gamma \bar{I}_i$ for proportional load sharing (satisfying the conditions (9)) are not identical unless $\alpha_i = c/\bar{I}_i$ for some constant $c \in \mathbb{R}$. Hence, the economic dispatch (13) is a more versatile objective that includes load sharing (4) as a special case.

VI. Secondary Integral Control

The primary droop control (7) results in a generally non-zero steady-state voltage drift given in (8) which has to be compensated by means of a secondary controller. In the following we investigate two secondary integral control strategies: a fully decentralized one and a distributed one.

A. Decentralized Integral Control

To compensate the steady-state voltage drift (8), we augment every droop controller (7) with a local integral control penalizing voltage drifts. The resulting PI droop control is

$$I_i^S = I_i^* - C_i \dot{V}_i^S - p_i \tag{17a}$$

$$D_i \dot{p}_i = \dot{V}_i^S \tag{17b}$$

where p_i is an integral control variable, and $D_i > 0$ is a gain. Notice that (17) is identical to (6), which in steady-state gives the conventional DC droop control (5). The decentralized integral controller (17) (and equivalently conventional DC droop control (5)) successfully corrects for the steady-state voltage drifts but fails to recover the desired injections for proportional load sharing and economic optimality.

Theorem 6.1: (Performance of decentralized integral control) *Consider the closed-loop secondary-controlled microgrid* (1) *with the decentralized integral controller* (17)*. Then the following statements hold:*
(**1**) *All source voltages* $V_i^S(t)$ *converge to stationary values without drift.*
(**2**) *The steady-state source injections do generally not achieve proportional load sharing* (4)*.*
(**3**) *The steady-state source injections are generally not optimal with respect to the economic dispatch problem* (13)*.*

B. Distributed Consensus Filter

Since the decentralized proportional controller (7) as well as the decentralized integral controller (17) cannot simultaneously achieve the desired injections while regulating the voltage drifts, we now focus on *distributed* secondary integral control strategies that are able to achieve the desired optimal injections at the requirement of communication.

The previous decentralized integral controller (17) results in the stationary injection $I_i^S = I_i^* - p_i(t \to \infty)$ which generally depend on initial values, expogeneous disturbances, and unknown load parameters and do not necessarily satisfy the optimality condition (15) of identical marginal costs. Hence, we propose the following *distributed consensus filter* to force an alignment of the marginal injection costs $\alpha_i p_i$:

$$I_i^S = I_i^* - C_i \dot{V}_i^S - p_i \tag{18a}$$

$$D_i \dot{p}_i = C_i \dot{V}^S - \sum\nolimits_{j=1}^{m} B_{ij} \left(\alpha_i p_i - \alpha_j p_j\right) \tag{18b}$$

where $D_i > 0$ and the terms $B_{ij} = B_{ji} \geq 0$ induce an undirected and connected communication graph among the sources $\mathcal{V}_s$. The consensus filter (18) resembles the distributed averaging PI (DAPI) controller proposed in [12] and combines the integral action (17) together with a consensus flow [18]. Given a communication network among the sources, the distributed consensus filter (18) regulates of the voltage drifts while recovering the desired injections for proportional load sharing or economic optimality.

Theorem 6.2: (Performance of distributed consensus filter) *Consider the closed-loop secondary-controlled microgrid* (1) *with the distributed consensus filter* (18)*. Then the following statements hold:*
(**1**) *All source voltages* $V_i^S(t)$ *converge to stationary values without drift.*
(**2**) *The steady-state source injections achieve proportional load sharing* (4) *if the controller gains are chosen as in* (9)*.*
(**3**) *The steady-state source injections are optimal with respect to the economic dispatch problem* (13) *if the controller gains are chosen as in* (16)*.*

VII. Simulation Results

We illustrate the performance of our proposed controllers in a simulation scenario. We consider the microgrid displayed in Fig. 1, where $\mathcal{V}_S = \{a,\ b,\ c\}$ and $\mathcal{V}_L = \{d,\ e,\ f,\ g,\ h\}$. The microgrid is operating in islanded mode, and the dashed blue lines indicate the communication topology among the controllers in the distributed consensus filter (18). To achieve proportional load sharing, the droop coefficients C_i are chosen proportional to the source capacities $\bar{I}$ as in (9). At $t = 10s$ the initial load demand $I^L = [-1,\ -2,\ -3,\ -3,\ -2]^T$ changes instantaneously to $I^L = [-4,\ -0.5,\ -1.5,\ -5,\ -0.5]^T$. We investigate the transient and stationary behavior of the closed loop using different control strategies; see Fig. 3.

The simulation results using primary droop control (7) are shown in Fig. 3(a). The constant voltage drifts ($\dot{v}_{\text{drift}}$) are visible as nonzero and identical (in steady state) slopes in Fig. 3(a), and the load sharing ratios ($I_i^S/\bar{I}_i$) converge to the same steady-state value, i.e., the load is shared proportionally. Fig. 3(b) shows the simulation results using decentralized integral control (17).The source voltages converge to constant values without drifts, but the load sharing ratios do not converge to the same steady-state values. Additionally, the red injection

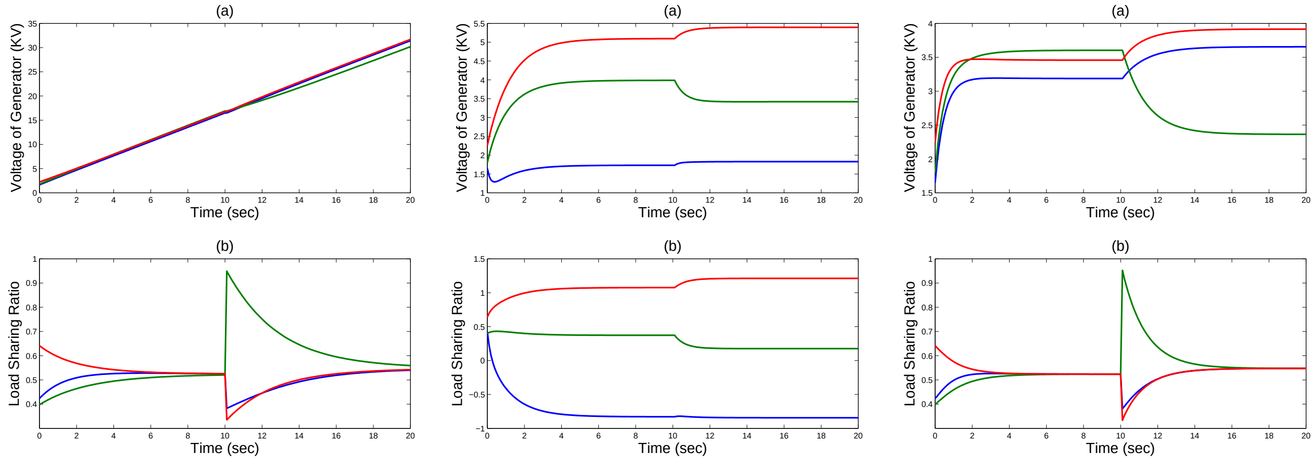

(a) Primary droop control (7). (b) Decentralized integral control (17). (c) Distributed consensus filter (18).

Fig. 3. Closed-loop performance of the microgrid under different control strategies

in Fig. 3(b) exceeds the value 1, that is, the associated source injection exceeds its capacity. Moreover, the blue injection in Fig. 3(b) shows that, the current injection is negative at steady state, that is, the associated source is absorbing (instead of supplying) current, which reveals another disadvantage of decentralized integral control. The simulation results using the distributed consensus filter (18) are shown in Fig. 3(c). Observe that the source voltages converge to constant values without drifts, and the load sharing ratios converge to the same values. Hence, the voltage drifts are regulated and proportional load sharing is achieved. Finally, note the different scales in the plots which indicate a superior transient performance of the distributed consensus filter (18).

VIII. Conclusions

Starting from the conventional DC voltage droop controller, we proposed novel decentralized and distributed primary droop and secondary integral control strategies for DC microgrids. We analyzed the properties and limitations of these control strategies, and investigated their consistencies with tertiary-level objectives such as proportional load sharing and an economic dispatch among the generating units. This work is a first step towards establishing an operation architecture for DC microgrids. In our initial setup, we assumed the loads to draw a constant current, and we considered purely resistive networks or networks with lines modeled by the resistive-capacitive Π-model. In future work we plan to study different network models including resistive-inductive-capacitive lines and ZIP load models.

IX. Acknowledgements

The authors wish to thank A. Davoudi and M. Andreasson for their comments and suggestions to improve the paper.

References

[1] J. M. Guerrero, J. C. Vasquez, J. Matas, L. G. de Vicuna, and M. Castilla, "Hierarchical control of droop-controlled AC and DC microgrids–a general approach toward standardization," *IEEE Transactions on Industrial Electronics*, vol. 58, no. 1, pp. 158–172, 2011.

[2] D. Nilsson and A. Sannino, "Load modelling for steady-state and transient analysis of low-voltage dc systems," in *Industry Applications Conference, 2004. 39th IAS Annual Meeting. Conference Record of the 2004 IEEE*, vol. 2, pp. 774–780 vol.2, Oct 2004.

[3] J. J. Justo, F. Mwasilu, J. Lee, and J.-W. Jung, "Ac-microgrids versus dc-microgrids with distributed energy resources: A review," *Renewable and Sustainable Energy Reviews*, vol. 24, no. 0, pp. 387 – 405, 2013.

[4] Q. Shafiee, T. Dragicevic, J. Vasquez, and J. Guerrero, "Modeling, stability analysis and active stabilization of multiple dc-microgrid clusters," in *Energy Conference (ENERGYCON), 2014 IEEE International*, pp. 1284–1290, May 2014.

[5] Y. Ito, Y. Zhongqing, and H. Akagi, "Dc microgrid based distribution power generation system," in *Power Electronics and Motion Control Conference, 2004. IPEMC 2004. The 4th International*, vol. 3, pp. 1740–1745, IEEE, 2004.

[6] D. Salomonsson and A. Sannino, "Low-voltage dc distribution system for commercial power systems with sensitive electronic loads," *Power Delivery, IEEE Transactions on*, vol. 22, pp. 1620–1627, July 2007.

[7] L. Xu and D. Chen, "Control and operation of a dc microgrid with variable generation and energy storage," *Power Delivery, IEEE Transactions on*, vol. 26, no. 4, pp. 2513–2522, 2011.

[8] V. Nasirian, S. Moayedi, A. Davoudi, and F. Lewis, "Distributed cooperative control of dc microgrids," *Power Electronics, IEEE Transactions on*, vol. 30, pp. 2288–2303, April 2015.

[9] M. Andreasson, D. V. Dimarogonas, H. Sandberg, and K. H. Johansson, "Control of MTDC Transmission Systems under Local Information," *ArXiv e-prints*, June 2014.

[10] D. Zonetti, R. Ortega, and A. Benchaib, "Modeling and Control of High-Voltage Direct-Current Transmission Systems: From Theory to Practice and Back," *ArXiv e-prints*, June 2014.

[11] F. Dörfler, J. Simpson-Porco, and F. Bullo, "Breaking the Hierarchy: Distributed Control & Economic Optimality in Microgrids," *ArXiv e-prints*, Jan. 2014.

[12] J. W. Simpson-Porco, F. Dörfler, and F. Bullo, "Synchronization and power sharing for droop-controlled inverters in islanded microgrids," *Automatica*, vol. 49, no. 9, pp. 2603–2611, 2013.

[13] J. Zhao and F. Dörfler, "Distributed control and optimization in DC microgrids," 2014. Submitted.

[14] P. Karlsson and J. Svensson, "Dc bus voltage control for a distributed power system," *Power Electronics, IEEE Transactions on*, vol. 18, pp. 1405–1412, Nov 2003.

[15] F. Dörfler and F. Bullo, "Kron reduction of graphs with applications to electrical networks," *IEEE Transactions on Circuits and Systems I: Regular Papers*, vol. 60, no. 1, pp. 150–163, 2013.

[16] A. Ostrowski and H. Schneider, "Some theorems on the inertia of general matrices," *Journal of Mathematical analysis and applications*, vol. 4, no. 1, pp. 72–84, 1962.

[17] S. Boyd and L. Vandenberghe, *Convex Optimization*. Cambridge University Press, 2004.

[18] F. Bullo, J. Cortés, and S. Martínez, *Distributed Control of Robotic Networks*. Princeton University Press, 2009.